Proton-Neutron and Proton-Proton Correlations in Medium-Weight Nuclei and the Role of the Tensor Force

M. Alvioli and C. Ciofi degli Atti

Department of Physics, University of Perugia and Istituto Nazionale di Fisica Nucleare, Sezione di Perugia, Via A. Pascoli, I-06123, Italy

H. Morita

Sapporo Gakuin University, Bunkyo-dai 11, Ebetsu 069, Hokkaido, Japan

(Received 6 December 2007; published 25 April 2008)

A detailed analysis of the effect of short-range and tensor correlations on one- and two-nucleon momentum distributions of medium-weight nuclei ($12 \leq A \leq 40$) is carried out. Although our Letter is primarily aimed at understanding the role of the tensor force on nucleon momentum distributions of medium-weight nuclei, the possible relevance of our results for the interpretation of $(e, e'N)$ and $(e, e'2N)$ processes at high Q^2, aimed at investigating nucleon-nucleon correlations, is discussed.

DOI: 10.1103/PhysRevLett.100.162503 PACS numbers: 21.30.Fe, 21.60.−n, 24.10.Cn, 25.30.−c

Obtaining information on short-range nucleon-nucleon correlations (SRC) in nuclei is a primary goal of modern nuclear physics. The interest in SRC stems not only from the necessity to firmly establish the limits of validity of the standard model of nuclei, but also from the strong impact that the knowledge of SRC in ordinary nuclei would have on other fields of physics, like, e.g., nuclear physics of stars and astrophysics. In fact, when the distance between two nucleons is about 1 fm, the local density of such a pair is comparable to the density expected in neutron stars; short-range correlated NN pairs represent therefore a form of cold dense nuclear matter that can be approached and studied in the laboratory. Such a study, in particular, the isospin dependence of SRC, would help to answer several crucial questions about the formation and the structure of neutron stars [1]. Recently, evidence of SRC has been provided by new experimental data on lepton and hadron scattering off nuclei at high-momentum transfer ($Q^2 \gtrsim 1$ GeV^2). The claimed evidence of SRC in these experiments resulted from the following. (i) The observation of a scaling behavior of the ratios of inclusive $A(e, e')X$ cross sections on heavy nuclei to those of the deuteron [2], for values of the Bjorken scaling variable $1.4 \lesssim x_{Bj} \lesssim 2$, and to those of ^{3}He [3], for $2 \lesssim x_B \lesssim 3$; this has been interpreted as evidence that the electron probes two- and three-nucleon correlations in nuclei similar to the ones in the two- and three-body systems; (ii) the observation of np pairs emitted back-to-back in the process $^{12}\mathrm{C}(p, ppn)X$ [4], which provided direct measurement of correlated np pairs, with a yield consistent with the $A(e, e')X$ results; a recent analysis of this experiment [5], based upon the two-nucleon correlation (2NC) model [6–8], demonstrates the dominance of pn SRCs over pp SRCs and provides the first experimental evidence of the isospin dependence of NN SRCs; (iii) the direct observation of pp correlated pairs in a recent JLab experiment [9], where a simultaneous measurement of the triple, $^{12}\mathrm{C}(e, e'pp)X$, and double, $^{12}\mathrm{C}(e, e'p)X$, coincidence reactions revealed that the probability ratio of $^{12}\mathrm{C}(e, e'pp)X$ to $^{12}\mathrm{C}(e, e'p)X$ events, for proton missing momenta above 300 MeV/c, is $(9.5 \pm 2)\%$. This experiment confirms the previous findings of [4] that the center-of-mass motion of a correlated pair has a behavior as predicted in [8]. Experimental work is planned [10], aimed at measuring the ratios $^4\mathrm{He}(e, e'pp)/^4\mathrm{He}(e, e'p)$, $^4\mathrm{He}(e, e'pn)/^4\mathrm{He}(e, e'p)$, and $^4\mathrm{He}(e, e'pn)/^4\mathrm{He}(e, e'pp)$ in the missing momentum range 500–875 MeV/c, in order to investigate the hard core region. The experimental results cited above stimulated new theoretical work in the field of SRCs. From one side, new theoretical approaches to the treatment of final state interactions (FSI) in $(e, e'p)$ and $(e, e'pN)$ processes, based upon improved eikonal approximations, have been developed [11] and applied [11,12] to the interpretation of the $(e, e'p)$ and $(e, e'pp)$ off few-nucleon systems. From the other side, the role of the tensor force in producing a substantial difference between pn and pp two-nucleon momentum distributions in few-body systems and light nuclei ($A \leq 8$) has been demonstrated [13] using state-of-the-art realistic nuclear wave functions obtained within the variational Monte Carlo (VMC) approach [14]. In this Letter the results of calculations of the one- and two-nucleon momentum distributions of medium-weight nuclei ($12 \leq A \leq 40$) will be presented (for preliminary results see [15]). Our approach is based upon a linked and number conserving cluster expansion [16] with correlated wave functions of the type $\Psi = \hat{F}\Phi$, where $\hat{F} = \prod \hat{f}_{ij}$ is a correlation operator generated by realistic interactions and Φ is a mean field (MF) wave function. Within this approach, the nondiagonal one-body density matrix (OBDM) at first order of the expansion reads as follows:

$$\rho^{(1)}(\boldsymbol{r}_1, \boldsymbol{r}_1') = \rho^{(1)}_{\mathrm{MF}}(\boldsymbol{r}_1, \boldsymbol{r}_1') + \rho^{(1)}_{H}(\boldsymbol{r}_1, \boldsymbol{r}_1') + \rho^{(1)}_{S}(\boldsymbol{r}_1, \boldsymbol{r}_1'), \tag{1}$$

 © 2008 The American Physical Society

where $\rho^{(1)}_{\rm MF}(\boldsymbol{r},\boldsymbol{r}') = \sum_{\alpha\in F}\varphi^{\star}_{\alpha}(\boldsymbol{r})\varphi_{\alpha}(\boldsymbol{r}')$ is the MF OBDM, and $\rho^{(1)}_{H}$ and $\rho^{(1)}_{S}$ are the hole (H) and spectator (S) correlation contributions; the former takes into account the contributions arising from the correlation between the struck proton and a nucleon of the spectator system ($A-1$), whereas the latter represents the contribution arising from the statistical coupling of the struck proton with a correlated pair in the spectator system ($A-1$); the hole contribution affects the high-momentum part of the momentum distributions, whereas the spectator one mainly renormalizes the MF momentum distributions. The nondiagonal two-body density matrix (TBDM) can be written as follows:

$$\rho^{(2)}(\boldsymbol{r}_1,\boldsymbol{r}_2;\boldsymbol{r}'_1,\boldsymbol{r}'_2) = \rho^{(2)}_{\rm MF}(\boldsymbol{r}_1,\boldsymbol{r}_2;\boldsymbol{r}'_1,\boldsymbol{r}'_2) + \rho^{(2)}_{2b}(\boldsymbol{r}_1,\boldsymbol{r}_2;\boldsymbol{r}'_1,\boldsymbol{r}'_2) + \rho^{(2)}_{3b}(\boldsymbol{r}_1,\boldsymbol{r}_2;\boldsymbol{r}'_1,\boldsymbol{r}'_2) + \rho^{(2)}_{4b}(\boldsymbol{r}_1,\boldsymbol{r}_2;\boldsymbol{r}'_1,\boldsymbol{r}'_2), \quad (2)$$

where $\rho^{(2)}_{\rm MF}$ is the MF TBDM and the other terms represent the correlation contributions, with the subscripts $2b$, $3b$, and $4b$ denoting the number of "bodies" (nucleons) involved in the given contribution. It should be stressed that our number conserving approach rigorously satisfies the sequential conditions that link the various density matrices. In Fig. 1, for the purpose of illustration, a particular class of hole and spectator Mayer diagrams considered in our approach are shown; the total number of correlation diagrams we have considered for the evaluation of $\rho^{(1)}(\boldsymbol{r}_1,\boldsymbol{r}'_1)$ and $\rho^{(2)}(\boldsymbol{r}_1,\boldsymbol{r}_2;\boldsymbol{r}'_1,\boldsymbol{r}'_2)$ was 5 and 20, respectively. In the case of central correlations [and harmonic oscillator (HO) MF wave functions] analytic expressions of the diagonal TBDM are given in Ref. [17]; when noncentral correlations are considered, as in the present case, no analytic expressions can be given even using HO wave functions. The one-nucleon momentum distribution (ONMD) is the Fourier transform of the OBDM [Eq. (1)], viz.,

$$n(\boldsymbol{k}) = \frac{1}{(2\pi)^3}\int d\boldsymbol{r}_1 d\boldsymbol{r}'_1 e^{-i\boldsymbol{k}\cdot(\boldsymbol{r}_1-\boldsymbol{r}'_1)}\rho^{(1)}(\boldsymbol{r}_1,\boldsymbol{r}'_1), \quad (3)$$

whereas the Fourier transform of the TBDM [Eq. (2)] yields the two-nucleon momentum distribution (TNMD), which can be written in terms of relative, $\boldsymbol{k}_{\rm rel}$, and center-of-mass (c.m.), $\boldsymbol{K}_{\rm c.m.}$, momenta, as follows:

$$n(\boldsymbol{k}_{\rm rel},\boldsymbol{K}_{\rm c.m.}) = \frac{1}{(2\pi)^6}\int d\boldsymbol{r}d\boldsymbol{R}d\boldsymbol{r}'d\boldsymbol{R}' e^{i\boldsymbol{K}_{\rm c.m.}\cdot(\boldsymbol{R}-\boldsymbol{R}')}e^{i\boldsymbol{k}_{\rm rel}\cdot(\boldsymbol{r}-\boldsymbol{r}')} \times \rho^{(2)}(\boldsymbol{r},\boldsymbol{R};\boldsymbol{r}',\boldsymbol{R}'). \quad (4)$$

The relative, $n_{\rm rel}(\boldsymbol{k}_{\rm rel})$, and c.m., $n_{\rm c.m.}(\boldsymbol{K}_{\rm c.m.})$, momentum distributions can be obtained from Eq. (4) by integrating over $\boldsymbol{K}_{\rm c.m.}$ and $\boldsymbol{k}_{\rm rel}$, respectively. In numerical calculations we have considered the nuclei ^{4}He, ^{12}C, ^{16}O, and ^{40}Ca; the MF wave functions were chosen in the Saxon-Woods form, with parameters fixed by minimizing the ground state energy using the $AV8'$ interaction [18]; this means that proper combinations of central, tensor, spin, and isospin correlations have been considered. The results for the ONMD are presented in Fig. 2 where, for ^{16}O, the effects of noncentral correlations and a comparison with higher order calculations, e.g., the VMC [19] and the Fermi hypernetted chain (FHNC) [20] approaches, are shown

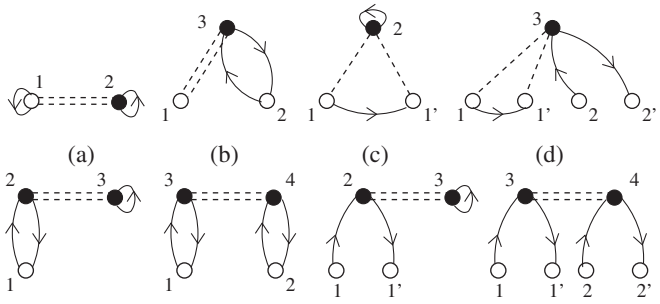

FIG. 1. Some (out of a total of 25) of the Mayer diagrams considered in the calculation of the diagonal (a),(b) and nondiagonal (c),(d) OBDM, Eq. (1), and TBDM, Eq. (2). Here, open dots denote the "active" particles, full dots labeled by an index "i" represent an integration over the coordinates of particle i, an oriented line originating and ending in the same dot denotes the mean field diagonal OBDM $\rho_o(i)$, whereas an oriented line joining two different dots denotes the nondiagonal OBDM, $\rho_o(i,j)$; the correlation operator ($\hat{\eta}_{ii'j} = \hat{f}_{ij}\hat{f}_{i'j} - 1$) is represented by dashed lines. Note that diagrams (a) and (b) are obtained from diagrams (c) and (d) by setting $1 = 1'$, $2 = 2'$, whereas diagrams (a) are obtained from diagrams (b) by integrating over particle "2". Upper (lower) diagrams belong to the class of *hole* (*particle*) diagrams.

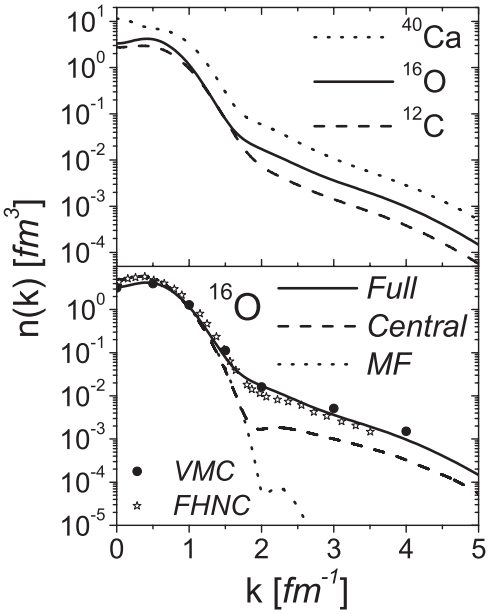

FIG. 2. Top: the ONMD [Eq. (3)] for ^{12}C, ^{16}O, and ^{40}Ca ($AV8'$ interaction [18]). Bottom: the MF and central correlation contributions to the momentum distribution of ^{16}O; the difference between the solid and dashed curves yields a measure of noncentral (mainly tensor) correlations. The results obtained within the cluster expansion (solid line) are compared with the VMC, Ref. [19] (full dots), and the FHNC, Ref. [20] (open stars). The normalization of the momentum distributions is $\int d\boldsymbol{k} n(k) = A$ [note that in Figs. 11 and 12 of Ref. [16] $n(k)$ is normalized to 1].

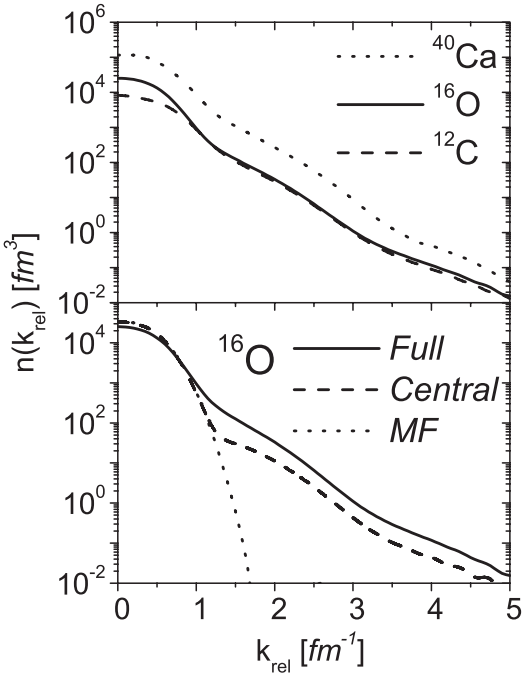

FIG. 3. Top: the relative TNMD [Eq. (4)] of ^{12}C, ^{16}O, and ^{40}Ca integrated over $\boldsymbol{K}_{\rm c.m.}$ ($AV8'$ interaction [18]). Bottom: the MF and central correlation contributions to the TNMD of ^{16}O. The normalization is $\int d\boldsymbol{k}_{\rm rel} n(k_{\rm rel}) = (2\pi)^6 A(A-1)/2$.

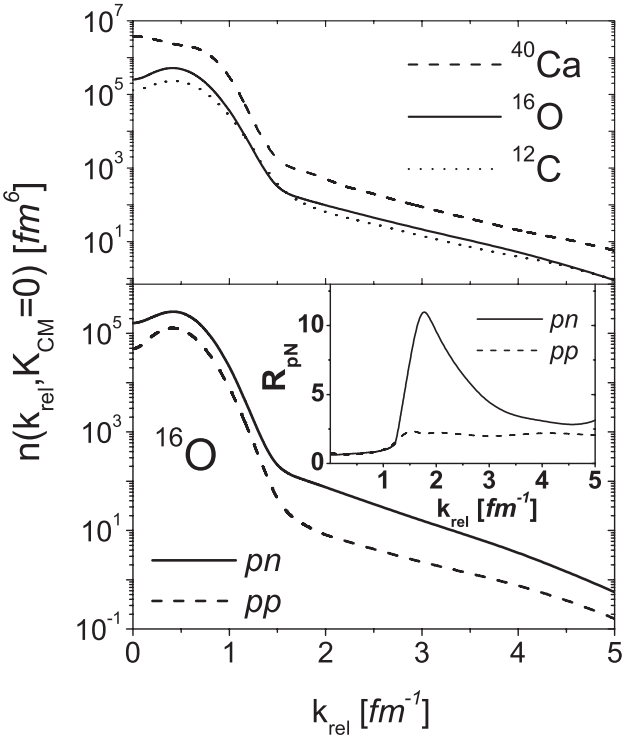

FIG. 4. Top: the relative TNMD [Eq. (4)] of ^{12}C, ^{16}O, and ^{40}Ca calculated in correspondence of $K_{\rm c.m.} = 0$ (back-to-back nucleons). Bottom: the pn and pp relative TNMD in ^{16}O for back-to-back nucleons [the total TNMD is given by $n(k_{\rm rel}, K_{\rm c.m.} = 0) = n_{pn}(k_{\rm rel}, K_{\rm c.m.} = 0) + 2n_{pp}(k_{\rm rel}, K_{\rm c.m.} = 0)$]. The inset shows the ratio $R_{pN} = n_{pN}(k_{\rm rel}, K_{\rm c.m.} = 0)/n_{pN}^{\rm central}(k_{\rm rel}, K_{\rm c.m.} = 0)$.

(the effect of higher order contributions within the linked cluster expansion has been shown to be a very tiny one [16]). The TNMD [Eq. (4)] integrated over $K_{\rm c.m.}$ are presented in Fig. 3 where, for ^{16}O, the MF contribution and the central and full (central plus noncentral) correlation contributions are shown. The TNMD corresponding to $K_{\rm c.m.} = 0$ (back-to-back nucleons) are presented in Fig. 4 where, for ^{16}O, the isospin separation of the total TNMD is illustrated by exhibiting the pp and pn pair contributions. In the same figure we also show the ratio $R_{pN} = n_{pN}(k_{\rm rel}, K_{\rm c.m.} = 0)/n_{pN}^{\rm central}(k_{\rm rel}, K_{\rm c.m.} = 0)$ where $N = (p, n)$; here n_{pN} includes both central and noncentral correlations, whereas $n_{pN}^{\rm central}$ includes central correlations only. It can be seen that in the region dominated by (tensor) correlations, the pn and pp ratios differ by about an order of magnitude. Eventually, we have evaluated the quantity

$$P_{pN} = \frac{\int_a^b dk_{\rm rel} k_{\rm rel}^2 n_{pN}(k_{\rm rel}, 0)}{\int_a^b dk_{\rm rel} k_{\rm rel}^2 [n_{pp}(k_{\rm rel}, 0) + n_{pn}(k_{\rm rel}, 0)]} \qquad (5)$$

representing the percentage probability of back-to-back pN pairs. We have considered the integration limits (in units of Fermis): $[a, b] = [0, \infty]$ and $[a, b] = [1.5, 3.0]$, the latter interval covering the region of high-momentum components originating from correlations. The calculated values of P_{pN} are shown in Table I. It can be seen that, in agreement with the result of Ref. [13], when the integration runs over the whole range of $k_{\rm rel}$, P_{pN} is proportional to the percentage of pN pairs, whereas the integration over the correlation region leads to a percentage of pn pairs much larger than that of the pp pair, which is a clear consequence of the effects of the tensor force acting between a proton and a neutron. The quantity P_{pN} of Eq. (5) refers strictly to back-to-back nucleons ($K_{\rm c.m.} = 0$). In Ref. [9], a simultaneous analysis of the ^{12}C$(e, e'p)$ and ^{12}C$(e, e'pp)$ reactions at $Q^2 = 2$ (GeV/c)^2, $x_B = 1.2$, led to the conclusion that in the range of missing momentum 1.5 fm$^{-1} \lesssim p_m \lesssim 3$ fm^{-1}, $(9.5 \pm 2)\%$ of the events observed in the $A(e, e'p)X$ process includes, besides the struck proton, a second backward emitted nucleon correlated partner of the struck nucleon with the c.m. motion of correlated pair described by a s-wave function with width as predicted in [8]. Therefore, we have calculated P_{pN} for different values of $K_{\rm c.m.} = 0.5$, 1, and 1.5 fm^{-1}, finding that the results listed in Table I change by only a few percent. This can be understood within the 2NC model, which assumes, for low values of $K_{\rm c.m.}$ and high values of

TABLE I. The pp and pn percentage probability [Eq. (5)] evaluated in the momentum range shown in square brackets.

A	P_{pp} (%) $[0, \infty]$	P_{pn} (%) $[0, \infty]$	P_{pp} (%) $[1.5, 3.0]$	P_{pn} (%) $[1.5, 3.0]$
4	19.7	81.3	2.9	97.1
12	30.6	69.4	13.3	86.7
16	29.5	70.5	10.8	89.2
40	31.0	69.0	24.0	76.0

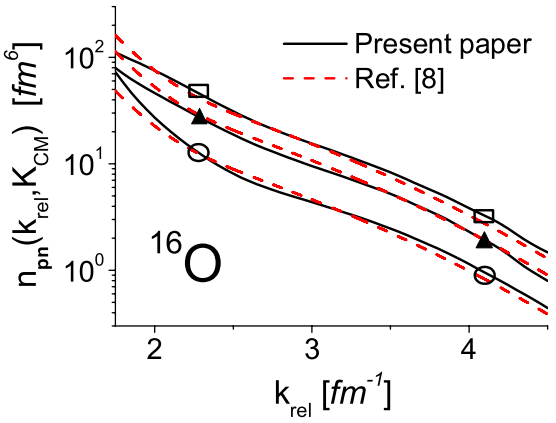

FIG. 5 (color online). Comparison of the many-body TNMD of this Letter [Eq. (4)] with the factorized form of Ref. [8] $n(\boldsymbol{k}_{\rm rel}, \boldsymbol{K}_{\rm c.m.}) = C_A n_D(k_{\rm rel}) n_{CS}(K_{\rm c.m.})$ (see text); the values of $K_{\rm c.m.}$ corresponding to the various curves are $K_{\rm c.m.} = 0$ fm^{-1} (squares), 0.5 fm^{-1} (full triangles), 1 fm^{-1} (open dots).

$k_{\rm rel}$, a factorization of the TNMD into the relative and c.m. momentum distributions [6–8]. As a matter of fact, as shown in Fig. 5, our many-body $n_{pn}(k_{\rm rel}, K_{\rm c.m.})$ in the region $1.5 \lesssim k_{\rm rel} \lesssim 2.0$ fm^{-1} and $0 \lesssim K_{\rm c.m.} \lesssim 1.0$ fm^{-1} fairly well factorizes as predicted in Refs. [6–8], into $n_{pn}^{\rm 2NC}(k_{\rm rel}, K_{\rm c.m.}) \simeq C_A n_D(k_{\rm rel}) n_{\rm c.m.}(K_{\rm c.m.})$, n_D being the deuteron momentum distribution, and $n_{\rm c.m.} = (2\pi\sigma^2)^{-3/2} \exp(-K_{\rm c.m.}^2/2\sigma^2)$ the c.m. momentum distribution, with $\sigma = 0.139$ GeV/c in agreement with the prediction of [8], confirmed by [4,5,9]. This is stringent evidence of the general validity of the 2NC model. In order to put this result on a more firm basis, one should estimate the P_{pN} probabilities starting, along the line of Ref. [5], from a calculation of the $(e, e'p)$ and $(e, e'pp)$ cross sections using one-body and two-body spectral functions taking FSI into account. Work is in progress and will be reported elsewhere. Concerning the dependence of P_{pN} upon the NN interaction model, we have estimated P_{pN} for ^{4}He using various types of interactions and found, as in Ref. [13], that interactions having the same tensor-to-central force ratio (e.g., $AV6'$, $AV8'$, $AV18$) affect very little the high-momentum part of the ONMD and TNMD and, consequently, the correlated values of P_{pN}.

To sum up, the main results we have obtained can be summarized as follows: (i) the high-momentum part of both the one- and two-nucleon momentum distributions in medium-weight nuclei is dominated by tensor correlations, which can reliably be described within the linked cluster expansion we have developed; (ii) in agreement with the results for light nuclei [13], at relative momenta $k_{\rm rel} \gtrsim 1.5$ fm^{-1}, the pn TNMD is much larger than the pp TNMD, whereas at small values of k_{rel} the ratio of pn and pp TNMD is proportional to the ratio of the number of pn to pp pairs; (iii) in the range 1.5 fm$^{-1} \lesssim k_{\rm rel} \lesssim 3$ fm^{-1}, thanks to the effect of the tensor force, the relative probability of having correlated pp and pn pairs in medium-weight nuclei is roughly $P_{pp} \simeq 10\%$ and $P_{pn} \simeq 90\%$, in apparent agreement with the findings of Refs. [4,5,9]: (iv) in the same region of relative momentum, calculations performed only with central correlations produce pp and pn probabilities proportional to the number of the corresponding pairs, i.e., $P_{pp} \simeq 30\%$ and $P_{pn} \simeq 70\%$; (v) in agreement with 2NC model predictions, the TNMD [Eq. (4)], calculated within our many-body approach exhibits, at large values of $k_{\rm rel}$ and low values of $K_{\rm c.m.}$, a clear factorized behavior.

Useful discussions with E. Piasetzky, R. Schiavilla, and M. Strikman are gratefully acknowledged. M. A. thanks the HPC-Europa project (No. RII3-CT-2003-506079) for a grant under the FP6 ''Structuring the European Research Area'' Programme, and H. M. thanks INFN and the Department of Physics, University of Perugia, for warm hospitality.

[1] M. M. Sargsian *et al.*, J. Phys. G **29**, R1 (2003).
[2] L. L. Frankfurt, M. I. Strikman, D. B. Day, and M. Sargsian, Phys. Rev. C **48**, 2451 (1993).
[3] K. S. Egiyan *et al.* (CLAS), Phys. Rev. Lett. **96**, 082501 (2006).
[4] A. Tang *et al.*, Phys. Rev. Lett. **90**, 042301 (2003).
[5] E. Piasetzky, M. Sargsian, L. Frankfurt, M. Strikman, and J. W. Watson, Phys. Rev. Lett. **97**, 162504 (2006).
[6] L. Frankfurt and M. Strikman, Phys. Rep. **76**, 215 (1981).
[7] C. Ciofi degli Atti, S. Simula, L. Frankfurt, and M. Strikman, Phys. Rev. C **44**, R7 (1991).
[8] C. Ciofi degli Atti and S. Simula, Phys. Rev. C **53**, 1689 (1996).
[9] R. Shneor *et al.*, Phys. Rev. Lett. **99**, 072501 (2007).
[10] E. Piasetzky and D. Higinbotham, JLab Experiment Report No. E07-006, 2007.
[11] M. Sargsian, T. V. Abrahamyan, M. Strikman, and L. Frankfurt, Phys. Rev. C **71**, 044614 (2005); **71**, 044615 (2005).
[12] C. Ciofi degli Atti and L. P. Kaptari, Phys. Rev. C **66**, 044004 (2002); C. Ciofi degli Atti and L. P. Kaptari, Phys. Rev. Lett. **100**, 122301 (2008).
[13] R. Schiavilla, R. B. Wiringa, S. C. Pieper, and J. Carlson, Phys. Rev. Lett. **98**, 132501 (2007).
[14] R. B. Wiringa and S. C. Pieper, Phys. Rev. Lett. **89**, 182501 (2002).
[15] M. Alvioli, C. Ciofi degli Atti, and H. Morita, in *Science and Supercomputing in Europe 2007*, edited by P. Alberigo, G. Erbacci, and F. Garofalo (CINECA, Bologna, Italy, 2007); arXiv:0709.3989v1.
[16] M. Alvioli, C. Ciofi degli Atti, and H. Morita, Phys. Rev. C **72**, 054310 (2005).
[17] S. S. Dimitrova, D. N. Kadrev, A. N. Antonov, and M. V. Stoitsov, Eur. Phys. J. A **7**, 335 (2000).
[18] R. B. Wiringa, V. G. J. Stocks, and R. Schiavilla, Phys. Rev. C **51**, 38 (1995).
[19] S. C. Pieper, R. B. Wiringa, and V. R. Pandharipande, Phys. Rev. C **46**, 1741 (1992).
[20] A. Fabrocini, F. Arias De Saavedra, and G. Có, Phys. Rev. C **63**, 044319 (2001).